DALTON
FULL PAPER

Electrochemical synthesis and structural characterisation of transition metal complexes with 2,6-bis(1-salicyloyl-hydrazonoethyl)pyridine, H_4daps

Manuel R. Bermejo,*[a] Matilde Fondo,[a] Ana M. González,[a] Olga L. Hoyos,[a] Antonio Sousa,*[a] Charles A. McAuliffe,*[b] Wasif Hussain,[b] Robin Pritchard[b] and Vladimir M. Novotorsev[c]

[a] *Departamento de Química Inorgánica, Facultad de Química, Universidad de Santiago, E-15706 Santiago de Compostela, Spain. E-mail: qimb45@uscmail.usc.es; qiansoal@uscmail.usc.es*
[b] *Department of Chemistry, University of Manchester Institute of Science and Technology, Manchester, UK M60 1QD*
[c] *N.S. Kurnakov Institute of General and Inorganic Chemistry, 31 Leninsky prosp., 117907 Moscow, Russian Federation*

Received 15th March 1999, Accepted 11th May 1999

Neutral manganese, cobalt and nickel complexes of the pentadentate hydrazone 2,6-bis(1-salicyloylhydrazono-ethyl)pyridine (H_4daps) have been prepared by means of electrochemical syntheses. They have been characterised by elemental analyses, IR spectroscopy, fast atom bombardment mass spectrometry (FAB) and magnetic susceptibility measurements. The molecular structures of $[Mn(H_2daps)(py)_2]$ **1**, $[Co(H_2daps)(py)_2]$ **2**, $[Ni_2(H_2daps)_2]\cdot CH_2Cl_2$ **3**, and $[Ni_2(H_2daps)_2(py)_2]\cdot CH_2Cl_2$ **4** have been determined by X-ray diffraction. Depending on the nature of the metal ion, the dianionic $[H_2daps]^{2-}$ ligand shows different co-ordination modes in these complexes: **1** and **2** are mononuclear with the metal atom in a pentagonal bipyramidal environment, **3** and **4** are binuclear with a helicate structure in which the nickel atoms attain octahedral co-ordination.

Introduction

In the past few years the co-ordination properties of hydrazone ligands have extensively been investigated.[1–9] The development of this co-ordination chemistry is, in part, the result of the interesting donor systems which could result. Many ligands, mainly containing nitrogen donors in heterocyclic rings, but also in hydrazones, have been investigated in an attempt to predict their behaviour upon co-ordination. The structural characterisation of the resultant mononuclear or polynuclear complexes has led to some emerging patterns and has improved the design of molecular threads which may be twisted, yielding helical molecular systems.[6,7] Nevertheless many questions still remain and the predicted systems are not always obtained. The desire for an in depth understanding of the rules that lead to systems of different nuclearity, together with their pharmacological activity,[10–12] as well as their interesting electric and magnetic properties,[13–15] make research on the co-ordination chemistry of hydrazone ligands even more attractive.

Part of our research program is directed towards the synthesis and structural characterisation of transition metal complexes with Schiff bases.[16] Many methods of synthesis have been tried in an attempt to obtain compounds of this kind. Recently we have turned our attention to electrochemical synthesis, as it has been found to be a convenient route for the preparation of neutral Schiff base metal complexes through the oxidation of a metal anode in a solution of a Schiff base bearing weakly acidic groups, *e.g.* salicylaldimines (phenol OH) or pyrrolaldimines (pyrrole NH).[17] In this paper we apply this methodology to synthesize neutral complexes of Mn, Co and Ni containing 2,6-bis(1-salicyloylhydrazonoethyl)pyridine, H_4daps with high purity and good yield.

Results and discussion

A series of neutral chelate complexes has been synthesized by electrochemical oxidation of the corresponding metal anode in the presence of the neutral ligand H_4daps in an organic solvent. The electrochemical efficiency of the cell (Table 1) was close to 0.5 mol F^{-1}, which is compatible with Scheme 1.

Table 1 Experimental conditions for the electrochemical syntheses (initial current 10.0 mA, electrolysis time 2.5 h)

Metal	Amount (mg) dissolved	Voltage (V)	E_f[a]/ mol F^{-1}
Mn	30.4	17.5	0.59
Co	30.2	4.2	0.55
Ni	25.1	3.3	0.52

[a] Electrochemical efficiency of the cell, defined as the amount of metal dissolved per Faraday of charge.

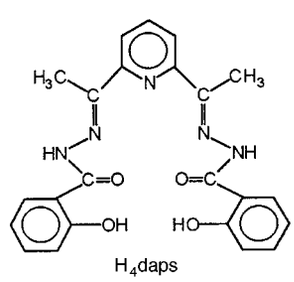

H_4daps

Cathode: $H_4daps + 2e^- \longrightarrow H_2(g) + H_2daps^{2-}$
Anode: $H_2daps^{2-} + M \longrightarrow M(H_2daps) + 2e^-$

Scheme 1

Elemental analyses (Table 2) show that all metals react with the ligand in molar ratio 1:1 to afford solvated complexes of the bis-deprotonated ligand $[H_2daps]^{2-}$ in high purity. These neutral metal complexes are obtained in high yields and appear to be stable in the solid state and in solution. Most of them are

Table 2 Analytical and some selected data for the complexes

Complex	Analysis (%)[a] C	N	H	μ_{eff}/μ_B	FAB[b] *m/z*	Colour
$Mn(H_2daps)(H_2O)_{0.5}$	56.0 (55.9)	14.4 (14.2)	3.6 (4.0)	5.7	485	Dark orange
$Co(H_2daps)(H_2O)_{1.5}(CH_3CN)$	54.3 (53.9)	14.9 (15.1)	4.4 (4.4)	4.0	489	Yellow-orange
$Ni(H_2daps)(H_2O)_{1.5}(CH_3CN)$	53.6 (53.9)	15.4 (15.1)	4.6 (4.5)	2.9	488–491; 976*	Yellow-brown
$Ni(H_2daps)(CH_2Cl_2)_{0.5}$	53.5 (53.2)	13.3 (13.2)	3.9 (3.8)	2.9	488–491; 976*	Yellow-brown

[a] Found (calculated). [b] Peaks corresponding to $[ML]^+$ except * that correspond to $[M_2L_2]^+$.

Table 3 Selected bond lengths (Å) and angles (°) for complexes **1** and **2** with estimated standard deviations (e.s.d.s) in parentheses

1		**2**			
Mn1–O2	2.243(4)	Co1–O2	2.153(5)	Co1–N2	2.210(6)
Mn1–N1	2.380(6)	Co1–O1	2.171(5)	Co1–N6	2.168(6)
Mn1–N2	2.267(5)	Co1–N1	2.213(6)	Co1–N7	2.193(6)
Mn1–N6	2.297(4)	Co1–N3	2.181(6)		
O2–Mn1–O2′	88.2(2)	O2–Co1–O1	78.3(2)	N1–Co1–N3	70.5(2)
O2–Mn1–N1	135.9(1)	O2–Co1–N1	140.2(2)	N1–Co1–N2	70.1(2)
O2–Mn1–N2	68.4(2)	O2–Co1–N3	149.2(2)	N1–Co1–N6	94.7(2)
O2–Mn1–N2′	156.1(2)	O2–Co1–N2	70.6(2)	N1–Co1–N7	88.6(2)
O2–Mn1–N6	87.6(2)	O2–Co1–N6	89.8(2)	N3–Co1–N2	140.1(3)
O2–Mn1–N6′	86.6(1)	O2–Co1–N7	87.6(2)	N3–Co1–N6	88.9(2)
N1–Mn1–N2	67.7(1)	O1–Co1–N1	141.2(2)	N3–Co1–N7	92.3(2)
N1–Mn1–N2′	67.7(1)	O1–Co1–N3	70.9(2)	N2–Co1–N6	88.3(2)
N1–Mn1–N6	94.0(1)	O1–Co1–N2	148.6(2)	N2–Co1–N7	92.8(2)
N2–Mn1–N2′	135.3(3)	O1–Co1–N6	88.1(2)	N6–Co1–N7	176.7(2)
N2–Mn1–N6	87.8(2)	O1–Co1–N7	89.4(2)		
N2–Mn1–N6′	95.2(2)				
N6–Mn1–N6	172.0(2)				

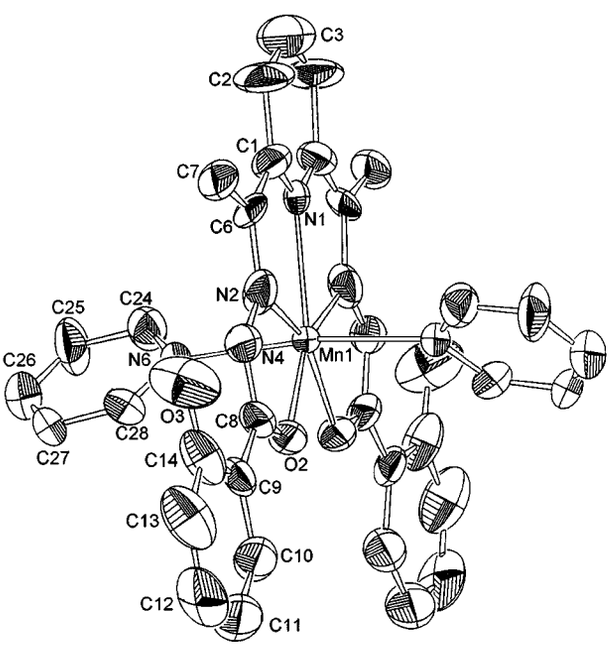

Fig. 1 Molecular structure of $[Mn(H_2daps)(py)_2]$ **1** showing the atomic numbering scheme.

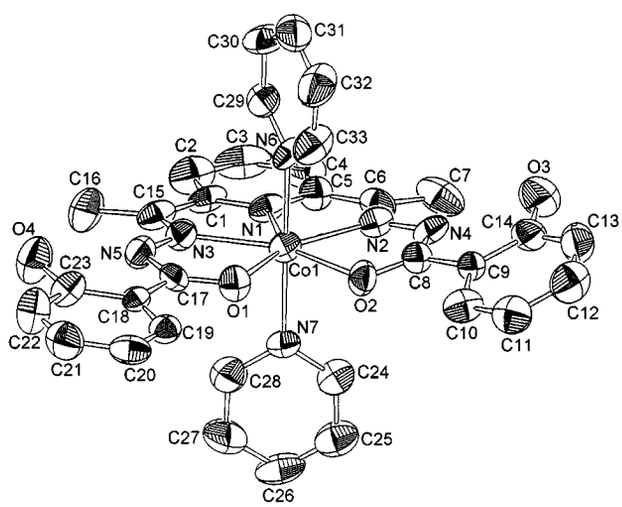

Fig. 2 Molecular structure of $[Co(H_2daps)(py)_2]$ **2** showing the atomic numbering scheme.

insoluble or sparingly soluble in water and common organic solvents but soluble in polar co-ordinating solvents such as DMF, DMSO and pyridine. All the complexes melt above 300 °C.

FAB mass and IR spectra

All the FAB mass spectra show peaks (Table 2) due to the fragments $[M(H_2daps)]^+$. A peak at *m/z* 976 due to the fragment $[Ni(H_2daps)]_2^+$ is also observed for **3** and for $Ni(H_2daps)(H_2O)_{1.5}(CH_3CN)$. The IR spectra show that in all cases the bands due to the amide I [ν(CO)] and amide II [δ(NH) + ν(CN)] modes undergo negative shifts of 19–60 and 46–64 cm^{-1}, respectively. This behaviour is compatible with the participation of the oxygen atoms of both carbonyl CO groups in the co-ordination to the metal, in agreement with previous results.[18] The spectra also show the absence of the ν(N–H) bands, which for the "free" ligand appear at 3208 cm^{-1}. This is in accordance with the dianionic nature of the ligand.

X-Ray studies

Crystal structures of $[Mn(H_2daps)(py)_2]$ 1 and $[Co(H_2daps)(py)_2]$ 2. The crystal structures of complexes **1** and **2** are shown in Figs. 1 and 2 and selected bond lengths and angles are given in Table 3. Both structures consist of discrete $[M(H_2daps)(py)_2]$ molecules, with a crystallographic twofold axis bisecting the

Table 4 Selected bond lengths (Å) and angles (°) for complexes **3** and **4** with estimated standard deviations (e.s.d.s) in parentheses

3				**4**			
Ni1–N1	2.281(5)	Ni2–N1	2.454(4)	Ni1–N1	2.175(11)		
Ni1–N1′	2.430(4)	Ni2–N1′	2.300(4)	Ni1–N2	1.990(12)		
Ni1–N4	1.962(4)	Ni2–N2	1.956(4)	Ni1–O1	2.120(10)		
Ni1–N4′	1.965(4)	Ni2–N2′	1.953(4)	Ni2–N4	2.136(13)		
Ni1–O2	2.026(4)	Ni2–O1	2.002(3)	Ni2–N5	2.148(12)		
Ni1–O2′	2.010(3)	Ni2–O1′	2.019(4)	Ni2–O3	2.036(10)		
Ni1 · · · Ni2	3.06(2)			Ni1 · · · Ni2	4.51(9)		
N4–Ni1–N4′	174.34(18)	Ni2–N1–Ni1	89.74(13)	N2–Ni1–N2′	165.1(7)	O3–Ni2–N4′	89.4(5)
N4–Ni1–O2′	106.31(16)	N2–Ni2–O1	79.10(17)	N2–Ni1–O1	76.9(4)	O3–Ni2–N4	87.4(5)
N4–Ni1–O2	79.35(16)	N2–Ni2–O1′	100.08(17)	N2–Ni1–O1′	93.0(4)	O3–Ni2–O3′	175(6)
N4–Ni1–N1	76.14(18)	N2–Ni2–N1′	104.37(17)	N2–Ni1–N1′	76.7(5)		
N4–Ni1–N1′	100.53(16)	N2′–Ni2–N2	173.70(17)	N2–Ni1–N1	113.1(5)		
N4′–Ni1–O2′	79.35(16)	N2′–Ni2–O1	107.14(16)	O1–Ni1–O1′	95.1(5)		
N4′–Ni1–O2	99.86(16)	N2′–Ni2–O1′	79.06(17)	O1–Ni1–N1′	153.6(4)		
N4′–Ni1–N1	104.64(17)	N2′–Ni2–N1′	75.80(17)	O1–Ni1–N1	87.5(4)		
N4′–Ni1–N1′	73.81(16)	N1–Ni2–N2	73.92(16)	N1′–Ni1–N1	101.7(6)		
O2′–Ni1–O2	104.37(15)	N1–Ni2–N2′	99.80(16)	N4–Ni2–N4′	87.9(7)		
O2′–Ni1–N1	84.49(15)	N1–Ni2–N1′	98.64(17)	N4–Ni2–N5	162.5(5)		
O2′–Ni1–N1′	153.05(14)	N1–Ni2–O1	152.73(17)	N4–Ni2–N5′	85.0(4)		
O2–Ni1–N1	155.14(15)	N1–Ni2–O1′	80.86(16)	N5–Ni2–N5′	106.0(6)		
O2–Ni1–N1′	82.80(15)	O1–Ni2–O1′	108.04(15)	O3–Ni2–N5	76.5(4)		
N1–Ni1–N1′	99.88(15)	O1–Ni2–N1′	84.17(15)	O3–Ni2–N5′	106.2(5)		
Ni2–N1–Ni1	80.73(14)	O1′–Ni2–N1′	154.41(15)	O3′–Ni2–N4′	87.4(5)		

molecule in complex **1**. The metal atom is in a distorted pentagonal bipyramidal environment $[MN_5O_2]$ in both complexes. The equatorial plane of the bipyramid is occupied by the N_3O_2 donor set of the $[H_2daps]^{2-}$ ligand, giving rise to four five-membered chelate rings.

Four of the five angles subtended at Mn by adjacent equatorial atoms are slightly smaller than the value of 72° for an ideal pentagonal bipyramidal arrangement, ranging from 67.7(1) to 68.4(2)°, while the fifth angle [O2–Mn1–O2′] is 88.2(2)°. The pentagon is less distorted in the cobalt complex [four angles ranging from 70.1 to 70.9° and the fifth O2–Co1–O1 78.3(2)°]. The deviations of the pentagon from planarity are also somewhat different in the two cases. The five atoms of the donor set are planar within the experimental errors for the manganese complex (maximum deviation from the N_3O_2 least squares plane = 0.084 Å, with the manganese atom sitting on the plane) while the deviation from planarity is slightly higher for the cobalt compound (maximum = 0.098 Å, with the cobalt atom 0.004 Å below this plane). In both cases the apical positions are filled by two pyridine molecules, which come from the solvent of crystallisation. The interaxial angle is closer to the ideal value in the cobalt (176.7(2)°) than in the manganese complex (172.0(2)°).

The structures of complexes **1** and **2** feature intramolecular hydrogen bonds between the phenol hydrogen atom and the hydrazide nitrogen atom, O (phenol) · · · N (hydrazide) of *ca.* 2.5 Å for the manganese and cobalt complexes. This interaction resulted in O3–C14 acquiring some double bond character (1.323(8) Å for Mn and 1.331(9) Å for Co; ideal value for C–OH (phenol) = 1.36 Å). These data are in agreement with the bis-deprotonated nature of the ligands in **1** and **2**.

All the angles and bond distances are similar to the values found in related seven-co-ordinate complexes of Co and Mn containing acylhydrazones [19–23] and do not merit further discussion. Intermolecular interactions by π–π stacking between two very close capping pyridines and between two phenol rings are observed in **1** but not in **2**.

Crystal structure of $[Ni_2(H_2daps)_2]\cdot CH_2Cl_2$ 3. The crystal structure of $[Ni_2(H_2daps)_2]\cdot CH_2Cl_2$ is shown in Fig. 3, together with the atom numbering scheme. Bond angles and distances are contained in Table 4. The compound is a binuclear nickel complex, with a helicate structure, solvated with one dichloromethane molecule. Each H_4daps behaves as a dianionic ligand

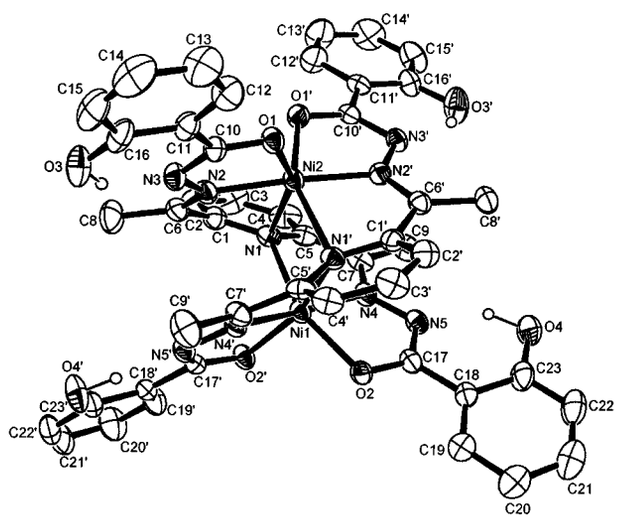

Fig. 3 An ORTEP[24] view of the crystal structure of $[Ni_2(H_2daps)_2]\cdot CH_2Cl_2$ **3**. Thermal ellipsoids are drawn at the 30% probability level. Lattice CH_2Cl_2 is not depicted. Hydrogen atoms, except those attached to oxygen atoms, are omitted for clarity.

using five [ONNNO] donor atoms, *viz.* the pyridine nitrogen, both imine nitrogen and both carbonyl oxygen atoms, as in **1** and **2**. However, the co-ordination mode of the ligand is found to differ from that in **1** and **2**. In **3** each ligand uses one imine nitrogen atom and one carbonyl oxygen atom to bind one metal centre. A rotation around the C–C bond adjacent to the pyridine ring allows the pyridine nitrogen atom to act as a bridge between the two nickel atoms. A further rotation about the symmetrical adjacent C–C bond leads to chelation of the remaining imine nitrogen and carbonyl oxygen atoms to a second metal centre, generating a double helical structure. This co-ordination mode produces four five-membered chelate rings around each nickel atom, which are in a distorted octahedral environment $[NiN_4O_2]$. The Ni · · · Ni distance is 3.06(2) Å. This short distance is the result of the distortion of the central rhombus Ni1–N1–Ni2–N1′, formed by both pyridine bridges and the two nickel atoms, with higher angles around each Ni atom (*ca.* 100°) and smaller than 90° around the pyridine nitrogen atoms.

The Ni–N bond lengths are rather different from one

another; the Ni–N (imine) bonds (of *ca.* 1.96 Å) are shorter than the Ni–N (pyridine) bonds [ranging from 2.281(5) to 2.454(4) Å]. For each metal ion, one of the Ni–N (pyridine) bond lengths [Ni1–N1 2.281(5) and Ni2–N1′ 2.300(4) Å] is shorter than the other one [Ni1–N1′ 2.430(4) Å and Ni2–N1 2.454(4) Å]. The shorter distance corresponds to the interaction between the nickel atom and the pyridine ring in an equatorial plane and the longer one to the interaction with the pyridine group in an axial position. The Ni–O distances are similar for both metals (*ca.* 1.27 Å) and do not deserve further consideration. The four C–N (imine) bond distances are *ca.* 1.28 Å, typical of a double C=N bond, and show the lack of electronic delocalisation as a consequence of the non-planar conformations of the ligands. The N (hydrazide)···O (phenol) distances of *ca.* 2.5 Å, typical of intramolecular hydrogen bonds, indicate deprotonation of the hydrazide nitrogen atoms of the ligand.

The most interesting feature of this compound lies in the octahedral environment around each metal centre and the double helical structure, as hydrazone ligands of this type usually lead to seven-co-ordinated complexes with a pentagonal bipyramidal geometry,[1–4,11–15] as has also been found in **1** and **2**. Helicates containing pyridine as a bridge have previously been described, mainly containing ligands with nitrogen donor atoms in heterocyclic rings or in acyclic imines,[7] but few of them contain hydrazones. As far as we know, the most similar complex reported is $[Ni(dapz)]_2$[25] [H_2dapz = 2,6-diacetylpyridinebis(1′-phthalozinylhydrazone)] and a comparison between bond distances and angles for both complexes is shown below (see Table 5).

Another important fact in relation with this structure is that it was thought that if a metal ion with a strong ligand field-imposed preference for an octahedral geometry was selected, and a ligand with central pyridine and two other bidentate domains in each thread was used, a double helicate would result.[7] The only difficulty would be to prevent the metal centres from adopting a pentagonal bipyramidal geometry. This could be avoided by introducing bulky substituents on the hydrazone. However these do not seem to be the unique reasons for obtaining a double helicate. The structure of a monomeric nickel compound $[Ni(H_4daps)(H_2O)_2]^{2+}$, containing H_4daps as a neutral ligand, has been described.[26] The nickel atom is in a $[NiN_3O_4]$ pentagonal bipyramidal environment, H_4daps forming the equatorial plane and the water molecules filling the axial positions. The different structures observed in **3** and in $[Ni(H_4daps)(H_2O)_2]^{2+}$ cannot be attributed to the different charge of the ligand (dianionic and neutral), as similar monomers have been found for manganese complexes containing dianionic and neutral H_2dappc ligands (H_2dappc = 2,6-diacetylpyridinebis(picolinylhydrazone)].[20] In addition, reasons adducing different nuclearity based on acidity of the reaction medium[27] seem not to be valid in this case, as both compounds $[Ni_2(H_2daps)_2]\cdot CH_2Cl_2$ and $[Ni(H_4daps)(H_2O)_2][NO_3]_2$ were obtained in a neutral medium.

In an attempt to obtain the mononuclear neutral complex, **3** was treated with pyridine. This method has been previously reported to be successful for obtaining monomeric cobalt complexes with 2,2′:6′,2″:6″,2‴:6‴,2⁗-quinquepyridine ligands from binuclear complexes.[28] However, in this case the experiment led to asymmetric cleavage of the pyridine bridges, yielding another helicate binuclear compound $[Ni_2(H_2daps)_2(py)_2]\cdot CH_2Cl_2$, **4**.

Crystal structure of $[Ni_2(H_2daps)_2(py)_2]\cdot CH_2Cl_2$ 4. The molecular structure of $[Ni_2(H_2daps)_2(py)_2]\cdot CH_2Cl_2$ **4** is shown in Fig. 4, together with the atom numbering scheme and main bond distances and angles are given in Table 4. The compound is a binuclear nickel derivative, with the Ni atoms located on a crystallographic twofold axis. The $[H_2daps]^{2-}$ ligand spans both metal atoms, and each nickel atom is in a distorted octahedral

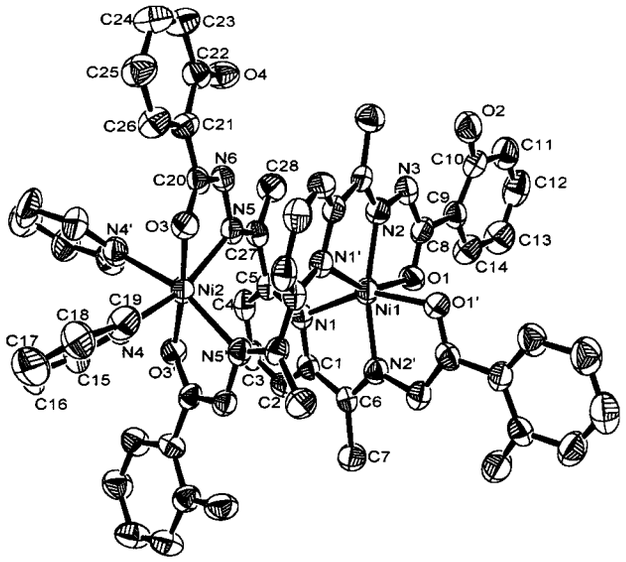

Fig. 4 An ORTEP view of the crystal structure of $[Ni_2(H_2daps)_2(py)_2]\cdot CH_2Cl_2$ **4**. Lattice CH_2Cl_2 is not depicted. Thermal ellipsoids are drawn at the 30% probability level.

$[NiN_4O_2]$ environment. However the nickel environments are different. One arises from co-ordination of one nickel atom to the pyridine nitrogen, the imine nitrogen and one carbonyl oxygen atom of two $[H_2daps]^{2-}$ ligands, the other from co-ordination of the nickel atom to one imine nitrogen and one carbonyl oxygen atom of two $[H_2daps]^{2-}$ ligands and to the two nitrogen atoms of two pyridine molecules.

Again, the Ni–N bond lengths are different from one another and, as in complex **3**, the Ni–N (imine) bonds are shorter than the Ni–N (pyridine) bonds. In addition, the Ni–N lengths corresponding to the isolated pyridine molecules are shorter than the one corresponding to the pyridine fragment of $[H_2daps]^{2-}$. This is most probably due to steric hindrance. It should be noted that these distances are shorter than the corresponding distances in **3**. This is a reflection of the pyridine in **3** acting as a bridging N donor rather than a terminal donor in **4**. The cleavage of the pyridine bridges also leads to a longer Ni···Ni distance in **4**, 4.51(9) Å, than in **3**, 3.06(2) Å.

The C–O (phenol) distances of 1.27(2) and 1.34(2) Å are shorter than the ideal value. These data and the distances N (hydrazide)···O (phenol) of *ca.* 2.5 Å suggest the presence of an intramolecular hydrogen bond between the phenol oxygen and the hydrazide nitrogen atoms, as a result of the bis-deprotonation of the ligand. It should be stressed that although the interaction of **3** with pyridine results is breaking of the pyridine bridges, the product of the reaction is not the expected mononuclear complex but a binuclear compound with both nickel atoms in different environments. This behaviour contrasts with the symmetric breaking of the pyridine bridges in a binuclear complex containing quinquepyridine ligands, to yield mononuclear compounds.[7,28]

If we compare the binuclear compounds **3** and **4** with the related complexes $[Ni_2(dapz)_2]$ and $[Ni(H_4daps)(H_2O)_2]^{2+}$ (Table 5), some conclusions can be drawn. (1) The complexes $[Ni_2(H_2daps)_2]$ and $[Ni_2(dapz)_2]$ present very similar double helical structures, with both hydrazone ligands adopting the same conformation. The most remarkable difference is a more distorted Ni1–N1–Ni2–N1′ central rhombus for **3**, leading to a shorter Ni–Ni distance (3.06(2) Å in **3** and 3.125(2) Å in $[Ni_2(dapz)_2]$). All the other distances are quite similar and in the range of those expected for complexes containing hydrazone ligands. (2) The comparison of **3** and **4** with $[Ni(H_4daps)(H_2O)_2]^{2+}$ is maybe more interesting and clearly shows a longer Ni–N (pyridine) distance in the binuclear complexes {ranging from 2.281(5) to 2.454(4) for **3**, 2.175(11) for **4** and 2.028(6) Å for $[Ni(H_4daps)$-

Table 5 Comparison of bond lengths (Å) in **3**, **4** and related complexes

	$[Ni(H_4daps)(H_2O)]^{2+}$ [a]	$[Ni_2(H_2dapz)_2]$ [b]	$[Ni_2(H_2daps)_2]$ [c]	$[Ni_2(H_2daps)_2(py)_2]$ [c]
Ni1–N (pyridine)	2.028(6)	2.347(7); 2.348(6)	2.430(4); 2.281(5)	2.175(11); 2.175(11)
Ni2–N (pyridine)	—	2.313(7); 2.249(6)	2.454(4); 2.300(4)	—
Ni1–N (imine)	2.194(6); 2.081(6)	1.985(7); 1.974(7)	1.965(4); 1.962(4)	1.990(12); 1.990(12)
Ni2–N (imine)	—	1.975(7); 1.967(7)	1.956(4); 1.953(4)	2.148(12); 2.148(12)
Ni1–O (carbonyl)	2.628(6); 2.247(6)	—	2.026(4); 2.010(3)	2.120(10); 2.120(10)
Ni2–O (carbonyl)	—	—	2.019(4); 2.002(3)	2.036(10); 2.036(10)
Ni1 · · · Ni2	—	3.125(2)	3.06(2)	4.51(9)
C–N (pyridine)	1.347(10); 1.319(11)	1.37(1); 1.36(1)	1.357(7); 1.345(6)	1.36(2); 1.34(2)
		1.36(1); 1.36(1)	1.364(7); 1.340(7)	1.36(2); 1.34(2)
C (pyridine)–C (imine)	1.490(11); 1.487(12)	1.48(1); 1.39(1)	1.481(8); 1.475(8)	1.50(2); 1.44(2)
		1.47(1); 1.45(1)	1.466(8); 1.460(8)	1.50(2); 1.44(2)
C–N (imine)	1.288(10); 1.275(10)	1.30(1); 1.30(1)	1.284(6); 1.279(6)	1.30(2); 1.30(2)
		1.30(1); 1.28(1)	1.288(7); 1.285(7)	1.30(2); 1.30(2)
N (imine)–N (hydrazine)	1.342(10); 1.332(10)	1.38(1); 1.36(1)	1.377(6); 1.373(6)	1.39(2); 1.39(2)
		1.38(1); 1.36(1)	1.375(6); 1.369(6)	1.39(2); 1.39(2)
N (hydrazine)–C (carbonyl)	1.371(11); 1.354(11)	—	1.342(7); 1.340(7)	1.35(2); 1.34(2)
			1.340(7); 1.327(7)	1.35(2); 1.34(2)
C–O (carbonyl)	1.221(10); 1.217(10)	—	1.276(6); 1.263(6)	1.28(2); 1.25(2)
			1.277(6); 1.266(6)	1.28(2); 1.25(2)
C–O (phenol)	1.377(9); 1.356(10)	—	1.346(7); 1.332(7)	1.34(2); 1.27(2)
			1.351(8); 1.335(8)	1.34(2); 1.27(2)
N (hydrazine) · · · O (phenol)	2.62(1); 2.58(1)	—	2.56(2); 2.54(2)	2.56(2); 2.56(2)

[a] Ref. 26. [b] Ref. 25. [c] This work.

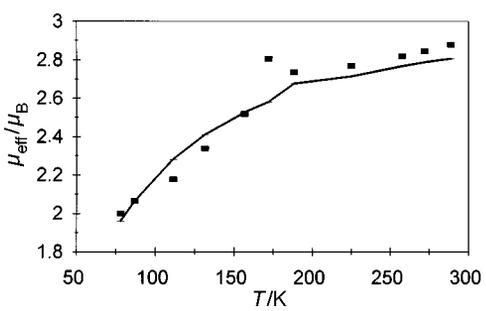

Fig. 5 Plot of effective magnetic moment *versus* T for complex **3**, in the range 78–300 K; ■ represents the experimental data and the solid line the best fit of the data.

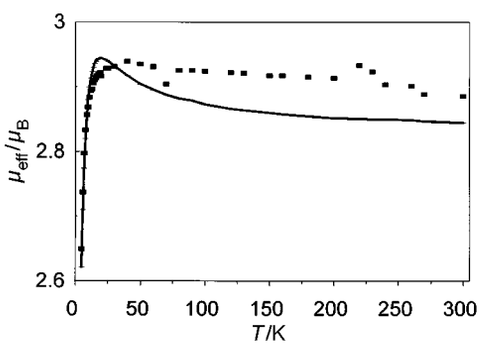

Fig. 6 Plot of effective magnetic moment *versus* T for complex **4**, in the range 5–300 K. Details as in Fig. 5.

$(H_2O)_2]^{2+}$}, even when the pyridine ring is acting as a terminal donor (**4**). In contrast to this, the Ni–N (imine) and Ni–O (carbonyl) bonds are shorter in the binuclear complexes. The non-planar conformation of the ligands and the consequent lack of delocalisation is shown in all cases by the short C–N (imine) bonds (*ca.* 1.28 Å). The dianionic nature of the ligand in **3** and **4** is pointed out by the C–O (phenol) distances: these are slightly shorter for the binuclear compounds and reflect the intramolecular hydrogen bond between the phenol oxygen and the hydrazide nitrogen atoms.

Magnetic measurements

All the compounds show magnetic moment values per atom very close to that expected for their magnetically dilute metal(II) ions at room temperature. This confirms the oxidation state +II of the metal centre and indicates the bis-deprotonation of H_4daps.

Magnetic measurements at variable temperature have been performed for the binuclear nickel compounds, **3** and **4**. Magnetic susceptibility data for **3** were collected in the 78–289 K range, using a Faraday balance, and in the 5–300 K range for **4** in a SQUID at a small applied field of 5000 G. The magnetic behaviour of **3** and **4** is shown in Figs. 5 and 6, respectively, as plots of μ_{eff} per Ni atom *versus* temperature.

The effective magnetic moments of complex **3** were calculated by formula (1). The value per Ni atom at room temperature is 2.88 μ_B and it decreases gradually with decreasing temperature, indicative of an antiferromagnetic exchange.

$$\mu_{eff} = (8\chi_M T)^{1/2} \quad (1)$$

The best fit of the values was obtained with the Heisenberg–Dirac–van Vleck (HDVV) theoretical model for two exchange-coupled nickel(II) ions in the absence of orbital degeneracy of the complex ground states. The spin Hamiltonian has the form (2) where J is the isotropic exchange coupling, g the isotropic g factor and S are the spins of the exchange coupled ions (in this case $S_1 = S_2 = 2$). The calculation of the theoretical μ_{eff} values and the least squares treatment were carried out as reported.[29] The best fit values are $-2J = 54$ cm^{-1}, $g = 2.2$ which are within the usual range expected for binuclear nickel(II) complexes, showing antiferromagnetic exchange. The amount of paramagnetic impurity is negligible within experimental error.

$$H = -2JS_1S_2 + g\beta H(S_{1z} + S_{2z}) \quad (2)$$

The effective magnetic moments of complex **4** *versus* temperature are shown in Fig. 6. The temperature dependency first increases with decreasing temperature and then passes through a maximum at 19 K, clearly indicating the existence of ferromagnetic exchange between the Ni atoms. The experimental results were fitted using eqn. (3). The isotropic spin Hamiltonian has the form (4) where α is the molar fraction of magnetic

$$\chi = (1 - \alpha)\chi_{dim} + \alpha_{mon} + N_\alpha \quad (3)$$

$$H = -2JS_1S_2 - 2zJM_s\langle Sz\rangle \quad (4)$$

Table 6 Crystal data and details of refinement for complexes **1**–**4**

	1	**2**	**3**	**4**
Formula	$C_{33}H_{29}MnN_7O_4$	$C_{33}H_{29}CoN_7O_4$	$C_{47}H_{38}Cl_2N_{10}Ni_2O_8$	$C_{28.5}H_{31}ClN_6NiO_6$
M	642.57	646.60	1059.19	647.75
Crystal system	Monoclinic	Monoclinic	Triclinic	Monoclinic
Space group	$C2/c$	$P2_1/n$	$P\bar{1}$	$C2/c$
a/Å	18.528(1)	14.315(8)	12.739(3)	20.993(4)
b/Å	12.783(7)	13.67(1)	14.266(3)	20.649(4)
c/Å	14.274(1)	16.126(5)	14.699(3)	16.821(3)
α/°	—	—	77.00(3)	—
β/°	112.36(5)	106.82(3)	84.61(3)	122.32(2)
γ/°	—	—	63.04(3)	—
V/Å^3	3126.7(5)	3021(5)	2139.9(9)	6162(2)
T/K	296(2)	296(2)	293(2)	293(2)
Crystal size/mm	0.40 × 0.25 × 0.25	0.30 × 0.30 × 0.30	0.40 × 0.22 × 0.10	0.40 × 0.30 × 0.20
Z	4	4	2	8
μ/cm^{-1}	4.51	6.15	9.93	2.135
Reflections collected	2982	5810	3603	2791
No. unique reflections	2884 (R_{int} = 0.096)	5572 (R_{int} = 0.134)	3391 (R_{int} = 0.0161)	2791
R	0.061	0.043	0.036	0.123
R'	0.050	0.043	0.036	0.124

impurities, N_α refers to the temperature-independent paramagnetism (250×10^{-6} cm^3 mol^{-1} per Ni^{II}) and $2zJM_s\langle Sz\rangle$ describes the interbinuclear interaction;[30] S are the spins of the exchange coupled ions (in this case $S_1 = S_2 = 1$ without zero-field splitting for the binuclear complex). The values of the parameters obtained from non-linear fits of the experimental data by eqn. (3) are $-2J = 2.55$ and $g = 2.0$, and agree fairly well with previous results for ferromagnetic exchange between nickel(II) ions.[31] While antiferromagnetic interaction in binuclear nickel(II) complexes is often observed, the presence of a ferromagnetic exchange is quite unusual[31] and shows the very different exchange mechanism between **3** and **4**. This is in accordance with the very different environments around the nickel atoms in the two cases.

Conclusion

The electrochemical synthetic methodology has been shown to be a new and simple way to prepare first row transition neutral metal(II) complexes of hydrazone ligands with high purity and good yield. The same reaction conditions lead to complexes of different nuclearity (mononuclear and binuclear), suggesting that Ni has a low preference for a pentagonal bipyramidal geometry. It thus seems that the central ion plays a more important role in producing helicates than the ligand itself.

Previous results seemed to indicate that the presence of a good donor solvent could break the pyridine bridges in a double helical complex to give rise to monomeric compounds with a co-ordination number of seven. The reaction mechanism must be more complicated as the presence of pyridine is not able to convert helicate **3** into the expected monomer. The addition of pyridine does indeed break the pyridine bridges, as predicted, but rather than producing the expected monomer it yields another binuclear compound.

As a result, it appears that we must think about new reasons to explain which variables really favour the production of helicates and what are the reasons for retention of the helicate structure in some hydrazone complexes in the presence of strong donors.

Experimental

Chemicals

All solvents, 2,6-diacetylpyridine and salicylhydrazide are commercially available and were used without further purification. Metals (Ega Chemie) were used as *ca.* 2 × 2 cm^2 plates.

Physical measurements

Elemental analyses were performed on a Carlo Erba EA 1108 analyser. The NMR spectra were recorded on a Bruker WM-250 spectrometer using DMSO-d_6 as solvent, infrared spectra as KBr pellets on a Bio-Rad FTS 135 spectrophotometer in the range 4000–600 cm^{-1} and fast atom bombardment (FAB) mass spectra on a Kratos MS-50 mass spectrometer, employing Xe atoms at 70 keV in *m*-nitrobenzyl alcohol as a matrix. Room-temperature magnetic susceptibilities were measured using a Digital Measurement system MSB-MKI, calibrated using tetrakis(isothiocyanato)cobaltate(II). Measurements of the binuclear nickel complexes were taken by the Faraday technique in the range 78–289 K for **3** and in a SQUID using an applied field of 5000 G in the range 5–300 K for **4**.

Ligand preparation

The ligand H_4daps was prepared as previously described.[2] Its purity was checked by elemental analyses, ^{1}H NMR and IR spectroscopy. The yield was almost quantitative (Found: C, 64.1; H, 4.8; N, 16.1. Calc. for $C_{23}H_{21}N_5O_4$: C, 64.0; H, 4.9; N, 16.2%). ^{1}H NMR (DMSO-d_6): δ 2.50 (s, 6 H), 6.97–8.17 (m, 11 H), 11.51 (s, br, 2 H) and 11.80 (br, 2 H).

Syntheses of the complexes

The compounds were obtained using an electrochemical procedure.[17,32] An acetonitrile solution of the ligand containing about 10 mg of tetramethylammonium perchlorate, as supporting electrolyte, was electrolysed using a platinum wire as the cathode and a metal plate as the anode. The cell can be summarised as: Pt(−)|H_4daps + MeCN|M(+), where M stands for the metal. The synthesis is typified by the preparation of $Ni_2(H_2daps)_2(H_2O)_{1.5}(CH_3CN)$. A suspension (0.2 g, 0.464 mmol) of the ligand in acetonitrile (80 cm^3), containing 10 mg of tetramethylammonium perchlorate, was electrolysed for 2.5 h using a current of 10 mA. Concentration of the resulting solution to a third of its initial volume yielded a yellow-brown solid that was washed with diethyl ether and dried under vacuum. Crystallisation from dichloromethane–hexane produced dark red crystals of $[Ni_2(H_2daps)_2]\cdot CH_2Cl_2$, suitable for X-ray diffraction.

Slow evaporation of pyridine–dichloromethane solutions containing $Mn(H_2daps)(H_2O)_{0.5}$, $Co(H_2daps)(H_2O)_{1.5}(CH_3CN)$ and $[Ni_2(H_2daps)_2]\cdot CH_2Cl_2$ yielded crystals of $[Mn(H_2daps)(py)_2]$, $[Co(H_2daps)(py)_2]$ and $[Ni_2(H_2daps)_2(py)_2]\cdot CH_2Cl_2$, respectively, suitable for X-ray diffraction.

Crystallographic measurements

Crystal data and details of refinement are given in Table 6 for all the structures.

$[Mn(H_2daps)(py)_2]$ 1 and $[Co(H_2daps)(py)_2]$ 2. Data were collected using an Enraf-Nonius CAD-4 diffractometer for complex **1** and a Rigaku AFC6S diffractometer for **2**. The structures were solved by direct methods[33] and refined by full-matrix least squares on F^2. Lorentz-polarisation corrections were applied. Hydrogen atoms attached to oxygen atoms were located in the Fourier map and isotropically refined. All calculations were performed using the TEXSAN crystallographic software package.[34]

$[Ni_2(H_2daps)_2]\cdot CH_2Cl_2$ 3. Data were collected using a CAD-4 diffractometer. The structure was solved by direct methods and refined using Fourier techniques. Hydrogen atoms attached to oxygen atoms were located. Data processing and computation were carried out by using the SHELXL 97 program package.[35]

$[Ni_2(H_2daps)_2(py)_2]\cdot CH_2Cl_2$ 4. Data were collected using a Nicolet P-3 diffractometer. The crystals were extremely unstable under X-ray irradiation and we were unable to prevent decomposition (standards decay = 51%). This is the reason for the rather poor resolution of the structure. The structure was solved by direct methods[33a] and refined using Fourier techniques.[36]

CCDC reference number 186/1458.

See http://www.rsc.org/suppdata/dt/1999/2211/ for crystallographic files in .cif format.

Acknowledgements

The authors thank Xunta de Galicia (XUGA 20901B97) and Ministerio de Educación y Ciencia (Spain) (PB95-0827) for financial support.

References

1 D. Wester and G. J. Palenik, *Inorg. Chem.*, 1976, **15**, 755.
2 C. Pelizzi and G. Pelizzi, *J. Chem. Soc.*, *Dalton Trans.*, 1980, 1970.
3 C. Pelizzi, G. Pelizzi and F. Vitali, *J. Chem. Soc.*, *Dalton Trans.*, 1987, 177.
4 C. Carini, G. Pelizzi, P. Tarasconi, C. Pelizzi, K. C. Molloy and P. C. Waterfield, *J. Chem. Soc.*, *Dalton Trans.*, 1989, 289.
5 A. Bonardi, C. Carini, C. Merlo, C. Pelizzi, G. Pelizzi, P. Tarasconi, F. Vitali and F. Cavatorta, *J. Chem. Soc.*, *Dalton Trans.*, 1990, 2771.
6 E. C. Constable, *Tetrahedron*, 1992, **48**, 10013.
7 E. C. Constable, in *Comprehensive Supramolecular Chemistry*, eds. J. L. Atwood, J. E. D. Davies, D. D. McNicol, F. Vögtle, J. P. Sauvage and M. W. Hosseini, Pergamon, Oxford, 1996, vol. 9, p. 213.
8 K. Andjelkovic, Y. Ivanovic, S. R. Niketic, B. Prelesnik and V. M. Leovac, *Polyhedron*, 1997, **16**, 4221.
9 S. Abram, C. Maichle-Mössmer and U. Abram, *Polyhedron*, 1998, **17**, 131.
10 M. Carcelli, P. Mazza, C. Pelizzi, G. Pelizzi and F. Zani, *J. Inorg. Biochem.*, 1995, **57**, 43 and refs. therein.
11 A. Bacchi, A. Bonardi, M. Carcelli, P. Mazza, P. Pelagatti, C. Pelizzi, G. Pelizzi, C. Solinas and F. Zani, *J. Inorg. Biochem.*, 1998, **69**, 101.
12 A. R. Todeschini, A. L. P. De Miranda, K. C. M. Da Silva, S. C. Parrini and E. J. Barreiro, *Eur. J. Med. Chem.*, 1998, **33**, 189.
13 O. Kahn, *Angew. Chem.*, *Int. Ed. Engl.*, 1985, **24**, 834.
14 J. M. Williams, M. A. Beno, K. D. Carlson, U. Geiser, H. C. J. Kao, A. M. Kini, L. C. Porter, A. J. Schultz, R. J. Thorn, H. H. Wang, M.-H. Wanyho and M. Evain, *Acc. Chem. Res.*, 1988, **21**, 1.
15 R. Sumita, D. D. Mishra, R. V. Maurya and N. Nageswara, *Polyhedron*, 1997, **16**, 1825.
16 M. R. Bermejo, M. Fondo, A. García-Deibe, M. Rey, J. Sanmartín, A. Sousa, M. Watkinson, C. A. McAuliffe and R. G. Pritchard, *Polyhedron*, 1996, **15**, 4185; C. E. Hulme, M. Watkinson, R. G. Pritchard, C. A. McAuliffe, N. Jaiboon, B. Beagley, A. Sousa, M. R. Bermejo and M. Fondo, *J. Chem. Soc.*, *Dalton Trans.*, 1997, 1805; M. Watkinson, M. Fondo, M. R. Bermejo, A. Sousa, C. A. McAuliffe, R. G. Pritchard, N. Jaiboon, N. Aurangzeb and M. Naeem, *J. Chem. Soc.*, *Dalton Trans.*, 1999, 31.
17 M. L. Durán, J. A. García-Vázquez, J. Romero, A. Castiñeiras, A. Sousa, A. D. Garnovskii and D. A. Garnovskii, *Polyhedron*, 1997, **16**, 1707; J. A. García-Vázquez, J. Romero, M. L. Durán, A. Sousa, A. D. Garnovskii, A. S. Burlov and D. A. Garnovskii, *Polyhedron*, 1998, **17**, 1547.
18 A. Bonardi, C. Merlo, C. Pelizzi, G. Pelizzi, P. Tarasconi and F. Cavatorta, *J. Chem. Soc.*, *Dalton Trans.*, 1991, 1063.
19 M. Nardelli, C. Pelizzi and G. Pelizzi, *Transition Met. Chem.*, 1977, **2**, 35.
20 C. Pelizzi, G. Pelizzi, G. Predieri and S. Resola, *J. Chem. Soc.*, *Dalton Trans.*, 1982, 1349.
21 C. Pelizzi, G. Pelizzi, G. Predieri and F. Vitali, *J. Chem. Soc.*, *Dalton Trans.*, 1985, 2387.
22 T. J. Giordano, G. J. Palenik, R. Palenik and D. A. Sullivan, *Inorg. Chem*, 1979, **18**, 2445.
23 S. Ianelli, G. Minardi, C. Pelizzi, G. Pelizzi, L. Reverberi, C. Solinas and P. Tarasconi, *J. Chem. Soc.*, *Dalton Trans.*, 1991, 2113.
24 C. K. Johnson, ORTEP, report ORNL-5138, Oak Ridge National Laboratory, Oak Ridge, TN, 1976.
25 G. Paolucci, S. Stelluto, S. Sitran, D. Ajo, F. Benetollo, A. Polo and G. Bombieri, *Inorg. Chim. Acta*, 1992, **193**, 57.
26 C. Pelizzi, G. Pelizzi, S. Porretta and F. Vitali, *Acta Crystallogr.*, *Sect. C*, 1986, **42**, 1131.
27 A. Bino and N. Cohen, *Inorg. Chim. Acta*, 1993, **210**, 11.
28 E. C. Constable, *Prog. Inorg. Chem.*, 1994, **42**, 42.
29 Y. V. Rakitin and V. T. Kalinnikov, *Soviemennaya magnetokhimiya (Modern Magnetochemistry)*, Nauka, St. Petersburg, 1994, p. 272.
30 Y. V. Rakitin, V. M. Novotorsev, G. M. Larin, V. V. Zelentsov and V. T. Kalinnikov, *J. Struct. Chem.* (*USSR*), 1974, **15**, 881.
31 D. Volkmer, B. Hommerich, K. Griesar, W. Haase and B. Krebs, *Inorg. Chem.*, 1996, **35**, 3792.
32 C. Oldham and D. G. Tuck, *J. Chem. Educ.*, 1982, **59**, 420.
33 (*a*) G. M. Sheldrick, SHELXS 86, in *Crystallographic Computing*, eds. G. M. Sheldrick, C. Krueger and R. Goddard, Oxford University Press, 1985, p. 175; (*b*) P. T. Beurskens, DIRDIF, Direct Methods for Difference Structures, an automatic procedure for phase extension and refinement of difference structure factors, technical report 1984/1, Crystallography Laboratory, Toernooiveld, Nijmegen, 1984.
34 TEXSAN, Structure Analysis Package, Molecular Structure Corp., The Woodlands, TX, 1985.
35 G. M. Sheldrick, SHELXL 97 (SHELXS 97 and SHELXL 97), Programs for Crystal Structure Analyses, University of Göttingen, 1998.
36 G. M. Sheldrick, SHELXL 93, University of Göttingen, 1993.

Paper 9/02018G